Power Reduction Techniques for Multiple-Subcarrier Modulated Diffuse Wireless Optical Channels

Weiwei Kang, *Student Member, IEEE*, and Steve Hranilovic, *Senior Member, IEEE*

***Abstract*— In this paper, two novel techniques are proposed to reduce the average optical power in wireless optical multiple-subcarrier modulated (MSM) systems, namely in-band trellis coding and out-of-band carrier design. Data transmission is confined to a bandwidth located near DC. By expanding the signal set and coding over the increased degrees of freedom, an in-band trellis coding technique achieved an average optical power reduction up to 0.95 dBo over conventional MSM systems while leaving the peak optical power nearly unaffected. With a symbol-by-symbol bias, the received DC level can be detected to provide a degree of diversity at the receiver. In this manner, an additional average optical power reduction up to 0.50 dBo together with a peak power reduction of 0.46 dBo is achieved. Moreover, the unregulated bandwidth available in wireless optical channels is exploited and out-of-band carrier signals are designed outside the data bandwidth to reduce the average optical power. Average optical power reduction as high as 2.56 dBo is realized at the expense of 4 out-of-band carriers and an increase in the peak optical power. Finally, combining the three techniques achieves the best average optical power reduction of 2.63 dB optical.**

***Index Terms*— Wireless infrared channel, indoor diffuse infrared communication, optical intensity modulation, multiple-subcarrier modulation, trellis-coded modulation.**

I. Introduction

DIFFUSE indoor wireless optical channels are an exciting complement to existing radio frequency (RF) systems due to their low cost, high security and freedom from spectral licensing issues [1], [2]. The common problem of co-channel interference and multi-access interference in RF systems is eliminated since optical transmissions are blocked by opaque objects. Whereas the spectrum in RF channels is strictly licensed, the optical band is unlicensed worldwide, providing a potentially large bandwidth. However, multipath distortion in indoor wireless optical channels imposes a sharp bandwidth constraint and confines data transmission to a lowpass region [1]. Multiple-subcarrier modulated (MSM) wireless optical systems send data in this lowpass region directly, improving spectral efficiency at the expense of optical power efficiency [3]. However, in previous work the higher frequency bands are ignored since they are effectively filtered-out by the multipath channel. In this paper, higher frequencies are exploited and *out-of-band* signals are designed not to send information, but to reduce the average optical power in wireless optical systems. These out-of-band emissions are contained to a given room and do not contribute to co-channel interference, as in RF systems. Data transmission is confined to an *in-band* region at low frequencies around DC where the channel attenuation and noise power are low. Additional gains in average optical power are realized by coding over sequences of inputs.

In diffuse indoor wireless optical systems, data are modulated onto the instantaneous intensity of an optical carrier which is emitted over a wide solid angle and allowed to reflect from surfaces in the room. As a result, only non-negative signal amplitudes can be sent on the channel. Additionally, the peak transmitted amplitude must be limited due to the limited dynamic range of the transmitter. Eye and skin safety regulations require that the average amplitude, i.e., average optical power, also be constrained. As a result of these amplitude constraints the direct application of modulation from electrical channels is not possible.

Electrical MSM systems suffer from a high peak-to-average power ratio (PAPR) due to the addition of many independent frequency carriers. This results in nonlinear distortion due to clipping of the transmitted waveform. The reduction of the PAPR in electrical MSM systems has been studied using a variety of techniques, including the use of coding [4]–[6], reserved subcarriers [7], [8], parallel-combinatory multiple-subcarrier (PCMS) techniques [9] and tone-injection [10]. A comprehensive review of electrical PAPR reduction techniques can be found in [11]. Although these techniques reduce the PAPR effectively in electrical MSM systems, their direct application to reduce the average optical power of optical wireless MSM systems is often inefficient. It is important to note that the objective of these techniques is to reduce the variance in the squared envelope of an *electrical* signal rather than minimizing the amplitudes, i.e., optical intensities, directly. In order to achieve gains, the amplitude constraints of wireless optical channels must be considered explicitly in the design of algorithms.

In fiber optic systems, MSM techniques have been applied to improve the aggregate capacity of video distribution sys-

Paper approved by J. A. Salehi, the Editor for Optical CDMA of the IEEE Communications Society. Manuscript received November 5. 2006; revised March 21, 2007. This paper was presented in part at the 23rd Biennial Symposium on Communications, Dept. of Electrical and Computer Engineering, Queen's University, May 30 - June 1, 2006, Kingston, Canada and in part at the IEEE International Conference on Communications, Istanbul, Turkey, June 11 - 15, 2006. Weiwei Kang is currently with the Center for Information and Communications Technology Research, The Pennsylvania State University, University Park, PA.

The authors are with the Dept. Electrical & Computer Engineering, McMaster University, Hamilton, Ontario, Canada L8S 4K1 (e-mail: hranilovic@mcmaster.ca).

Digital Object Identifier 10.1109/TCOMM.2008.060609.

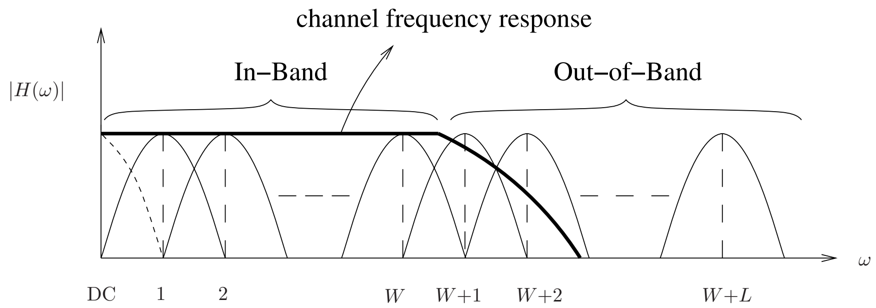

Fig. 1. Spectrum of an MSM wireless optical system using W in-band and L out-of-band carriers.

tems [12]. Carruthers and Kahn [3] first investigated MSM indoor wireless optical communications as a means to provide bandwidth efficient communication as well as multiple access. Independent data were transmitted on each in-band carrier and a fixed bias was added to each symbol to ensure non-negative amplitude. A time-varying bias signal was introduced in [13] as a means of both reducing the average optical power and improving detection. As in electrical systems, large positive and negative amplitude peaks may occur in optical MSM systems. The negative peaks require a large bias, and hence average optical power, to ensure non-negativity. This problem was first treated in [14] where optimized block codes were developed to reduce the average optical power in MSM systems with QPSK symbols. In [15], reserved subcarriers are added to the in-band BPSK signals and the transmitted amplitudes optimized to provide an average optical power reduction. The PCMS technique [9] was applied to wireless optical MSM systems by adding a symbol-by-symbol bias [16]. In [17], constellation point assignments over all carriers in a given symbol were chosen from a subset of MSM signals with low average optical power such that the minimum distance among each pair of codewords is maximized. Reference [18] provides an overview of optical intensity MSM techniques. A notable trend in previous work is that solely block coding was considered and no coding was applied over sequences of input symbols. Additionally, the reduction of both peak and average optical powers was not expressly treated.

In this work, we propose two main approaches to realize a gain in average optical power for MSM wireless optical systems: in-band coding and out-of-band carrier designs. In contrast with previous work, a trellis coding technique is developed to impose structure on *sequences* of in-band carrier symbols to realize a reduction in both peak and average optical power. Additionally, the DC bias used to ensure non-negativity is also used in code design and detected to provide an additional degree of diversity at the receiver. We also propose the use of carriers outside of the channel bandwidth to alleviate the average optical power constraint. Although others have considered the use of reserved subcarriers in RF and wireless optical channels, these carriers were added to the in-band carriers at a cost of reduced spectral efficiency. Our approach adds carriers at high frequencies outside of the data transmission bandwidth of the channel so that the spectral efficiency is unaffected. This approach is especially well suited to wireless optical channels since their spectra are unregulated and the inherent isolation of optical emissions does not cause interference with other users.

The paper is organized as follows. Section II describes a popular model for diffuse indoor wireless optical channels and introduces optical MSM systems. Section III presents our in-band trellis coding and DC detection technique. Two out-of-band carrier design techniques are introduced in Sec. IV and their complexities compared. Simulation results of the proposed techniques along with a comparison to existing techniques are given in Sec. V. The paper concludes in Sec. VI with some directions for future work.

II. Channel Model and Wireless Optical MSM System

A. Channel Model

Indoor diffuse wireless optical channels are well modelled by the following baseband linear system [1]

$$y(t) = rx(t) \otimes h(t) + n(t) \tag{1}$$

where $\otimes$ denotes convolution, r [A/W] is the photodetector responsivity, $x(t)$ [W] is the transmitted intensity-modulated signal, $h(t)$ is the channel impulse response, $n(t)$ [A] is the noise process and $y(t)$ [A] is the received photocurrent. Without loss of generality, we set $r = 1$ for the balance of this paper. The dominant noise source in indoor wireless optical channels is shot noise resulting from high-intensity ambient light. The noise is well modelled as being white, signal independent and Gaussian distributed with variance σ^2 [1].

Although multipath fading is not an issue in such channels due to the inherent spatial diversity of the receiver, multipath distortion resulting from multiple reflections within the room leads to a lowpass channel frequency response [1]. The bandwidth of the channel is on the order of $10 - 40$ MHz in most configurations [19], [20]. In this work we assume that the channel is flat in the bandwidth used for data transmission as shown in Fig. 1. This flat lowpass region of spectrum is termed the *in-band* region while all higher frequencies are termed *out-of-band*. Due to multipath distortion, the attenuation in the out-of-band region is high and signals transmitted in this band are heavily distorted at the receiver.

Since $x(t)$ is an optical power signal it must satisfy,

$$x(t) \geq 0. \tag{2}$$

The average optical power, P_a, must also be limited due to eye safety requirements. From (1), a constraint is placed on

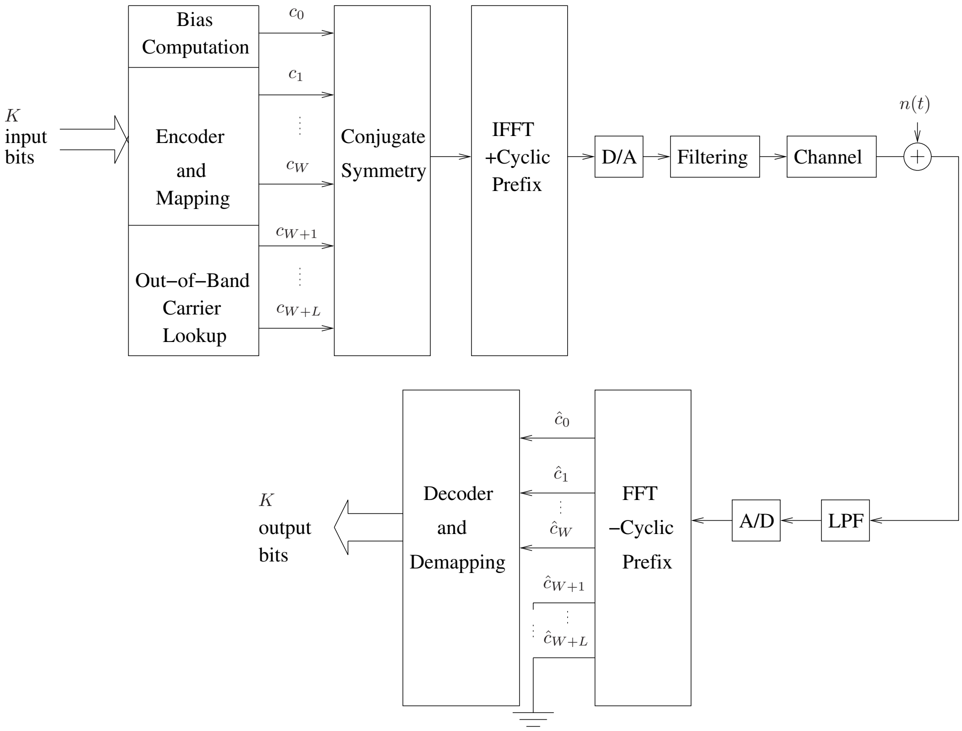

Fig. 2. MSM wireless optical system with out-of-band carriers.

the average amplitude

$$P_a = E[x(t)] \tag{3}$$

rather than $E[x^2(t)]$ as in electrical channels. Thus, a gain in optical power, in decibels, is equivalent to twice of that value in electrical dB. For example, a 1 dB improvement in average optical power corresponds to a 2 dB gain in electrical domain. Moreover, the maximum amplitude

$$P_p = \max_t \ x(t) \tag{4}$$

should also be limited due to the limited dynamic range of the transmitter.

B. Wireless Optical MSM System Definition

Consider an optical MSM system with W in-band and L out-of-band carriers, as in Fig. 1. Fig. 2 presents a diagram of the MSM system. On each of the W in-band carriers a complex information-bearing symbol, $c_1 \ldots c_W$, is transmitted while the complex values on the L out-of-band carriers, $c_{W+1} \ldots c_{W+L}$ are designed to reduce the transmitted average optical power. A bias, c_0, must also be transmitted to ensure non-negativity of the output signal. Sections III and IV discuss the design of the in-band encoder and out-of-band carriers respectively. It is assumed that the symbol period is limited to T seconds and that a rectangular window is employed. Since only real-valued signals can be transmitted, Hermitian, i.e., conjugate, symmetry must be preserved in the spectrum. The output waveform is generated by taking the inverse fast Fourier transform (IFFT) of the sequence and appending a cyclic prefix to ensure independence between carriers is preserved with transmission through the channel. The resulting MSM waveform transmitted is given by

$$\begin{aligned} x(t) &= \sum_k \mathrm{Re}\left[\sum_{i=0}^{W+L} c_i^k \exp\left(-j2\pi i(t-kT)/T\right)\right] \mathrm{rect}((t-kT)/T) \end{aligned} \tag{5}$$

where

$$\mathrm{rect}(t) = \begin{cases} 1 & : \quad t \in [0,1] \\ 0 & : \quad \text{otherwise} \end{cases}.$$

Notice that in order for $x(t)$ in (5) to satisfy the non-negativity constraint (2), the bias $c_0^k \in \mathbb{R}$ must be chosen appropriately. Consider selecting the minimum bias required to ensure non-negativity in each symbol interval, that is, $c_0^k = -\min_{t\in[0,T)} s^k(t)$ where

$$s^k(t) = \mathrm{Re}\left[\sum_{i=1}^{W+L} c_i^k \exp\left(-j2\pi i t/T\right)\right]. \tag{6}$$

Notice that $s^k(t)$ can be interpreted as the unbiased output from the W in-band and L out-of-band carriers. It has been shown that adding such a symbol-by-symbol bias offers significant optical power reduction [13], [14]. The average optical power (3) of the $x(t)$ is then,

$$P_a = E[x(t)] = E[c_0^k].$$

Thus, the goal of an optical power reduction technique is to reduce the expected magnitude of the required DC bias. The amplitudes selected on the W in-band and L out-of-band carriers are designed to minimize c_0^k and hence the average optical power of the wireless optical MSM system.

As shown in Fig. 2, the receiver performs the inverse of the transmitter by discarding the cyclic prefix and by performing a fast Fourier transform (FFT) on the sampled data. Again, it is assumed that the addition of the cyclic prefix has maintained the independence of signals amongst the carriers. In this work, the particular details of how the inter-carrier interference is eliminated between the carriers is not important as there are many techniques which can be applied. Notice that only the DC bin and the W data-bearing carriers are used by the decoder and that the out-of-band carriers are discarded. The out-of-band carriers do not carry independent information but are added to alleviate the amplitude constraints *at the transmitter*. It is important to note that the out-of-band carriers do not interfere with users in other rooms due to the inherent containment of diffuse infrared radiation.

C. Definitions

The bandwidth measure adopted in this paper is the null-to-null bandwidth, in accordance with previous work. The bandwidth of the transmitted signal is determined by T and the number of in-band carriers, W. Since the L out-of-band carriers are not required for detection and are contained to a given room, they are not considered in the bandwidth computation. Assuming K bits are sent per symbol period, the null-to-null bandwidth efficiency of the system is defined as

$$\eta = \frac{K}{W+1} \qquad \text{[bits/sec/Hz]}. \tag{7}$$

This measure is adopted as a fair metric of comparison for the schemes considered here since it quantifies the data rate for a given bandwidth cost, even in the presence of coding over the symbols.

To facilitate the comparison of average and peak optical power requirement of various techniques, define a reference rectangular on-off keying (OOK) wireless optical system with bit error rate (BER) 10^{-6}, average optical power P_{aOOK} and peak optical power P_{pOOK} as is conventionally done [1], [14]. As in [2], for this BER, $P_{\mathrm{aOOK}} = 4.75\sqrt{R_{\mathrm{OOK}}\sigma^2}$ where R_{OOK} is the bit rate of the reference system. Similarly, the peak optical power P_{pOOK} is given by $P_{\mathrm{pOOK}} = 2P_{\mathrm{aOOK}}$ and $\eta_{\mathrm{OOK}} = 1$ bit/s/Hz. The peak and average optical powers of all wireless optical MSM schemes considered are normalized by P_{aOOK} and P_{pOOK} respectively while operating at the same bit rate and BER as the reference OOK system to yield,

$$\rho = 10\log_{10}\frac{P_a}{P_{\mathrm{aOOK}}} \;\; \text{[dBo]}, \quad \psi = 10\log_{10}\frac{P_p}{P_{\mathrm{pOOK}}} \;\; \text{[dBo]} \tag{8}$$

where ρ is termed the *normalized average optical power* and ψ is the *normalized peak optical power*.

To conform with previous work in the area, we adopt in this paper the conventional term "normal MSM system" [14] to denote an optical MSM system with QPSK constellation employed on each carrier and a symbol-by-symbol bias.

III. In-band Optical Power Reduction Techniques

Consider the encoding and mapping blocks for the W in-band carriers in Fig. 2. This section presents an in-band coding technique to reduce the average optical power in wireless optical MSM systems. Unlike block coding considered in [14], the trellis coding technique presented here imposes a structure on sequences of MSM symbols. Finally, a DC detection technique is presented which exploits the signal-space diversity to realize a reduction in the average optical power.

A. Design of In-Band Trellis Codes

Inspired by Ungerboeck's work on coded modulation [21] and Frenger's work on PCMS [9], we expand the signal set for each carrier and develop trellis coded modulation over the increased degrees of freedom to realize gains in average optical power. The resulting system is termed trellis-coded MSM (TCMSM) in this paper and can achieve gains in average and peak optical power. As in [21], coded modulation system design includes constellation expansion, set partitioning, choice of trellis structure and a search for a mapping between constellation points and edges in the trellis.

1) MSM Constellations: Given an MSM wireless optical system with W in-band carriers, define a *sub-constellation* as the common constellation employed on each frequency carrier. In our scheme, each sub-constellation is expanded by adding a zero amplitude to a QPSK constellation or to an 8-PSK constellation, as is done in [9]. The resulting constellations are called 5-APSK and 9-APSK respectively. This constellation expansion increases the degrees of freedom available in choosing constellation points. Unlike earlier work [16], we do not transmit independent information on these degrees of freedom directly, but develop coded modulation to improve the optical power efficiency.

Further, define an *MSM constellation point* as an assignment of W sub-constellation points to each of the W in-band carriers. Trellis codes are designed in Sec. III-A.2 to exploit the added degrees of freedom to provide sequences of MSM constellation points with improved Euclidean distance. The cost of this technique is additional complexity in the form of a trellis encoder at the transmitter and a Viterbi decoder at the receiver.

Each MSM constellation point is constrained to have a zero amplitude on *at least* U carriers, $0 \leq U \leq W$, for *all* data symbols. For $U > 0$, this constraint is shown to enable a suboptimal search algorithm to find codes with lower average optical power requirements. In code design, each sub-constellation is partitioned to the lowest level where only a single constellation point is contained.

2) Code Design: A trellis structure is used to design sequences of MSM constellation points. Each trellis edge, determined by both the input bits and the current state, is mapped to an MSM constellation point. The trellis structure is fixed to have M states with at least one branch to each next state. If K bits are to be sent per symbol interval, each branch in the trellis must therefore send $K - \log_2 M$ bits using parallel transitions.

Given the trellis structure, the mapping between MSM constellation points and branches in the trellis determines the free Euclidean distance, d_{free}, of the code. The d_{free} asymptotically determines the error performance of the code and is the minimum distance for any error path leaving and returning to the all-zeros codeword. In this scheme, d_{free} can be limited by two MSM constellation points on the

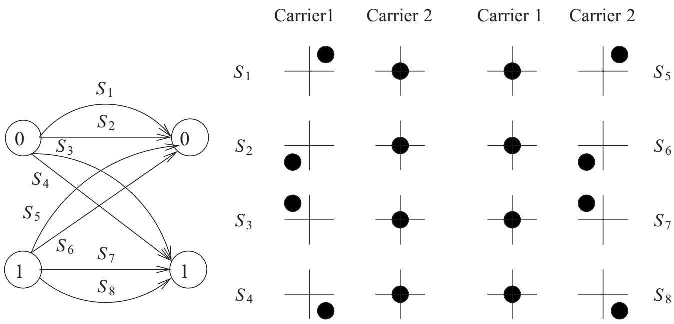

Fig. 3. Trellis structure and MSM constellation points for $K = 2$, $M = 2$, $W = 2$ and $U = 1$.

same branch or two different paths that start and end at the same state. Denote these distances as d_p and d_s respectively. Motivated by Ungerboeck's trellis code design heuristics [21], the following rules are applied when searching for a mapping:

1) Any MSM constellation point can occur only once at each stage of the trellis.
2) Maximize the distance between parallel edges, d_p.
3) Pick points on edges leaving or entering the same state with maximum d_s.

Rule 1 avoids confusion in decoding at each stage. Rules 2 and 3 are designed to maximize d_p and d_s respectively. Figure 3 presents a hand-designed example of a two state code ($M = 2$) satisfying the above heuristic and sending $K = 2$ bits per symbol using $W = 2$ in-band carriers with 5-APSK sub-constellations and constraint $U = 1$. The labels S_i refer to MSM constellation points. Notice that for all parallel edges, d_p is maximized subject to the $U = 1$ constraint. The remaining MSM constellation points are chosen to maximize d_s. At each stage of the trellis, given the current state, one input bit selects the next state while the other bit selects which of the MSM constellation points, i.e., edges S_i, to transmit. Note that these heuristics do not necessarily lead to an optimal code in any sense, but are designed to yield good performance.

To transmit K bits per symbol, the number of MSM constellation points assigned to each stage of the trellis is

$$n_\mathrm{input} = M2^K. \tag{9}$$

The number of possible mappings grows exponentially as n_input and any exhaustive search is prohibitively expensive even for small K. However, the search is greatly constrained if an MSM constellation point is selected at each step. Suppose at the fth step, $f - 1$ MSM constellation points have been assigned. Let $d_i, i \in [1, f-1]$ denote the Euclidean distances between the fth point and the ith assigned point. Define P_f as,

$$P_f = \sum_{d=d_1}^{d_{f-1}} Q\left(\frac{d}{2\sigma}\right),$$

where $Q(\cdot)$ is the Gaussian tail function. The function P_f is an upper bound on the a posteriori probability of error given the fth MSM constellation point was transmitted over the $f - 1$ assigned points. At each step, a point is chosen to minimize this upper bound. Using this intuition, the following sub-optimal search algorithm is used to find good mappings for the TCMSM system:

Algorithm Search for an MSM constellation point mapping for a given constraint $U \geq 0$.

1) Fix the first MSM constellation point.
2) For the fth MSM constellation point ($f > 1$), select the point with at least U zero points which minimizes P_f.
3) If the number of occurrences of current point $n > 1$, return to step 2 and pick the point with the next smallest P_f.
4) Fix current point, add 1 to the number of occurrences of this point. If assignment not finished, go to step 2.
End.

The search algorithm uses all possible starting points in step 1. At high rates, the number of all possible starting points is too large and 100 random starting points are selected. Note that the same search algorithm is implemented over both constrained constellations ($U > 0$) and unconstrained constellations ($U = 0$), despite the fact that the constrained constellation is a subset of the unconstrained constellation. In fact, the search over the constrained constellation often returned codes with a smaller average optical power requirement than search results over the more general unconstrained constellation. This is due to the sub-optimal search algorithm which improves the distance properties of the code stepwise rather than globally. Additionally, for each system the search is run using QPSK, 5-APSK and 9-APSK constellations for each non-zero in-band carrier. These constellations were chosen for their simplicity of implementation. However, as the number of phases increases, more freedom is allowed at the cost of increased time consumed by the search algorithm. The search terminates with a set of codes and the code with minimum average optical power at each bandwidth efficiency is chosen. The performance of TCMSM systems are shown in Sec. V.

B. DC Level Detection

The symbol-by-symbol bias used in MSM wireless optical systems is clearly correlated to the transmitted signal and provides additional information about the transmitted sequence. This correlated information can be exploited to provide a degree of signal space diversity, which improves the detection performance of the receiver [13]. The additional complexity required by DC detection is that joint detection over all in-band carriers and DC bin must be implemented as opposed to independent detection for each in-band carrier in normal MSM systems.

The DC bias required to ensure an MSM constellation point satisfies the non-negativity constraint can be used to increase the distance between MSM constellation points. The DC level of each MSM constellation point is computed and MSM constellation points including their DC distance are used in the search algorithm described in Sec. III-A.2. The difference in DC biases can be used to increase the distance between MSM constellation points and the search algorithms may return codes with larger d_free. However, due to the sub-optimal nature of the search, the inclusion of DC distance does not always return codes with larger d_free. In such cases, detection using the DC bias is employed solely at the receiver. The performance of this DC detection technique applied to TCMSM systems is shown in Section V.

It should be noted that this paper assumes an additive white Gaussian noise process. However, fluorescent light noise introduces larger noise power at low frequencies near DC [22]. In this case, the performance of the DC detection technique will be degraded and, in the worst case, no improvement in detection will be achieved, assuming the receiver has knowledge of the noise distribution and spectral density. Therefore, it is desirable to use the DC detection technique when the additional complexity at the receiver can be tolerated.

IV. Design of Out-of-Band Carrier Signals

The unregulated bandwidth in wireless optical channels can be exploited by adding carriers at out-of-band frequencies, as shown in Fig.1, and optimizing their amplitudes to reduce the average optical power at the transmitter. Notice that using out-of-band carriers does not incur a penalty in spectral efficiency, as is the case with previous approaches, since these frequencies are unregulated and are contained to a given room.

Out-of-band carrier symbol design need only be performed *once* for each MSM constellation point chosen and stored at the transmitter. The receiver has no knowledge of the out-of-band carriers and discards them before detection. Thus, the detector using out-of-band carriers is the same as a conventional MSM wireless optical receiver and each carrier can be decoded independently, yielding significant complexity savings. Therefore, this technique shifts the complexity from the receiver to the transmitter, where generation of out-of-band carriers and a lookup table to store the out-of-band carrier amplitudes are required.

Note that the out-of-band carrier design technique cannot be applied to RF systems since, unlike wireless optical systems, strict spectral masks are defined in these channels to limit interference with other communication schemes.

A. Optimization of Amplitudes Over the Complex Plane

In this section the results in [14], [15] are extended by finding the optimum amplitudes on the out-of-band carriers. For each MSM constellation point, the problem of finding the L optimum out-of-band carrier amplitudes to reduce the average optical power can be formulated as a convex optimization problem [23]. For a given MSM constellation point the W symbols $c_1, \ldots, c_W$ in Fig. 2 are specified. The minimum amplitude of $s(t)$ (6), or equivalently the required bias to ensure non-negativity, is estimated by discretizing it into samples $\{s_0, s_2, \ldots s_{A-1}\}$ where A is chosen so that the error in approximation is small. The optimization problem can then be formulated as follows,

$$\begin{aligned} \text{maximize} \quad & s_{\min} \\ \text{subject to } s_{\min} \le s_a, a = 0, 2 \ldots A-1 & \\ d_i = c_i \quad i \in [1, W] & \\ d_i \in \mathbb{C}, \quad i \in [W+1, W+L] & \\ s_a = \operatorname{Re}\left[\sum_{i=1}^{W+L} d_i \exp\left(-j2\pi i a/A\right)\right]. & \end{aligned}$$

This problem can be easily cast as a linear program and can be solved effectively using standard optimization algorithms. To bound the approximation error for a given A, an upper bound on the absolute value of the slope for each MSM constellation point is computed. An upper bound as well as a lower bound on the amplitude of the continuous waveform at time periods between any two samples is then computed. In simulations, $A = 1000$ which results in an approximation error of less than 0.01 dB.

The design is done once and the amplitudes for each MSM constellation point are stored at the transmitter. If single-precision floating point numbers are used to store the results in a table, 8 bytes are required to store the in-phase and quadrature amplitudes on each out-of-band carrier [24]. Given n_{input} possible input symbols, the memory requirement for L real-amplitude out-of-band carriers is

$$n_{\text{input}} \times L \times 8 \quad [\text{bytes}]. \tag{10}$$

where $n_{\text{input}} = 4^W$ for a normal MSM system and $n_{\text{input}} = M \times 2^K$ as in (9) for a TCMSM system.

Unlike previous work [14], [15], using out-of-band carriers does not reduce the bandwidth efficiency of the system. Moreover, the optimum amplitudes on L out-of-band carriers are found by solving the optimization problem. Section V presents the performance of this technique applied to the normal MSM system and the TCMSM system using $L = 1, 2, 3, 4, 10$ out-of-band carriers.

B. Optimization of Amplitudes Over a Discrete Constellation

A limitation of selecting amplitudes for the out-of-band carriers over a continuous set is the storage requirement at the transmitter. Consider that the L out-of-band carrier amplitudes are designed over a 9-APSK constellation to alleviate the transmitter memory requirement. For each data symbol, an exhaustive search over an 9-APSK constellation is performed once to find the optimal in-phase and quadrature amplitudes on the L out-of-band carriers which minimizes the average optical power. The number of possible amplitudes on L out-of-band carriers is 9^L for each data symbol, which makes an exhaustive search practical to implement for small L.

To improve the average optical power reduction capability, a real scaling factor α, in the range $(0, 1]$, is introduced to scale the amplitude transmitted on *all* out-of-band carriers with respect to the amplitudes of the in-band carriers. Unlike the most general case of individual complex values on each out-of-band carrier considered in Sec. IV-A, α is fixed for all symbols. To find a good value of α, the range of $(0, 1]$ is discretized into 20 points. For each α, the exhaustive search was performed to minimize the average optical power. Note that introducing α increases the size of the lookup table by 4 bytes.

The out-of-band 9-APSK symbols stored at the transmitter require one byte for each MSM constellation point. Thus, the memory requirement for L, 9-APSK out-of-band carriers and the α scaling factor is

$$n_{\text{input}} \times L + 4 \quad [\text{bytes}].$$

The memory required by restricting the out-of-band carriers to a scaled discrete constellation is asymptotically $1/8$ of that with no restriction for large n_{input}. Thus, this technique is

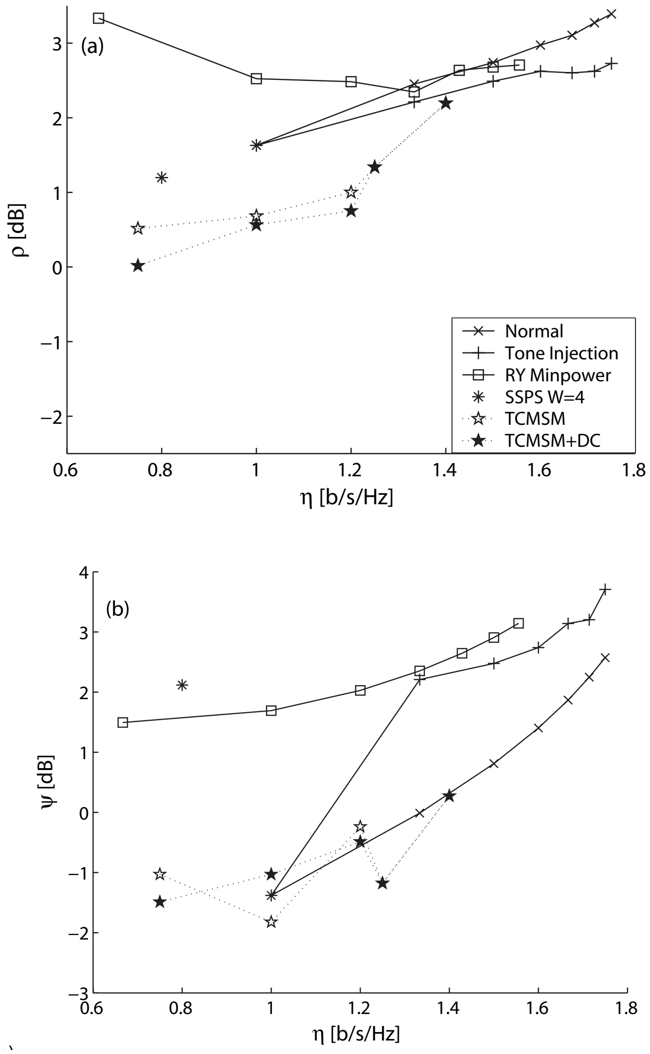

Fig. 4. In-band techniques: normalized average optical power (ρ) (a) and normalized peak optical power (ψ) (b) versus bandwidth efficiency (η) for normal MSM, tone injection [10], You block codes [14], SSPS [17] and TCMSM. Note the prefix 'DC' indicates results using DC bias detection technique.

more suitable for applications where the complexity of the transmitter must be limited.

The scaled 9-APSK out-of-band carrier technique proposed in this section differs from [14] in three aspects. Firstly, the carriers are located at the out-of-band region and using them does not affect the bandwidth efficiency of the system. Secondly, a scaling factor α is introduced to further reduce the average optical power. Lastly, the out-of-band carriers are chosen from 9-APSK constellation rather than a QPSK constellation. The performance of $L = 4$ discrete-constellation out-of-band carriers applied to the normal MSM system and the TCMSM system are presented in Sec. V

V. Simulation Results

Figures 4(a) and 4(b) plot the normalized average optical power ρ and the normalized peak optical power ψ defined in (8) of in-band techniques versus bandwidth efficiency η defined in (7). TCMSM codes are designed for $W = 2, 3, 4, 5$ for which the search algorithm is able to return results within a reasonable amount of time. For a given W, the rate of transmission is maximized by increasing K until the search algorithm fails to return codes with average optical power better than the normal system. For each pair of W and K, all possible combinations of $U = 0, 1, 2,\ M = 2, 4$ and choice of QPSK, 5- or 9-APSK constellations are considered, and the best codes are summarized in Tbl. I (for $L = 0$). Notice that the sub-constellation chosen in all cases is 9-APSK, illustrating that a higher degree of freedom in choosing the constellation points improves the performance of trellis codes. In fact, an improvement on the order of 0.5 dB was seen by using 9-APSK over QPSK. Although large constellations may yield further improvement, the search time required to find such codes increases greatly. The DC detection technique is also applied to TCMSM codes. For comparison, a normal MSM system is simulated for $W = 1, \ldots, 7$ and both the minimum-power block coding technique [14] and a recent SSPS code given in [17, Tbl. II] are presented. A popular PAPR reduction technique for electrical channels, tone injection [10], was also simulated in this application and the average and peak optical powers computed. All the systems are designed to have the same bit rate and BER of 10^{-6}.

In Fig. 4(a) it is evident that bandwidth efficiency is traded for average optical power efficiency for all power reduction schemes, as is conventional in optical signalling design [25]. All proposed systems outperform existing techniques at the same bandwidth efficiency. The in-band techniques operate well at low bandwidth efficiencies. The TCMSM code achieved a reduction up to 0.95 dB optical in average optical power while simultaneously *reducing* the peak optical power by 0.44 dB optical at $\eta = 1$. Notice that at higher η, the performance of in-band coding approaches that of the normal system. This is due to the fact that the degrees of freedom in code design were limited at high η since the search was carried out over at most $W = 5$ carriers due to the computational cost of the sub-optimal search procedure. It is anticipated that better codes at higher η could also be found using the same algorithm with $W > 5$ given additional computing resources. By applying DC detection to a TCMSM system, an additional average optical power reduction of up to 0.50 dB is achieved with a simultaneous peak power reduction of 0.46 dB at $\eta = 0.75$. It should be noted that the peak optical power of both in-band techniques are comparable to normal MSM systems but are not always reduced, as shown in Fig. 4(b). This is because the average optical power is the only criterion in the selection of codes at each bandwidth efficiency. Notice also that the average optical power of the tone injection algorithm, designed for electrical PAPR reduction, is significantly increased over TCMSM at low bandwidth efficiencies. Additionally, the peak requirement of this technique is large and comparable to the minimum power block coding technique at high η [14]. Thus, careful design of algorithms tailored to optical intensity MSM systems are required to realize large gains in power efficiency.

The performance of $L = 4$ out-of-band carriers applied to normal MSM systems is shown in Figs. 5(a) and 5(b). The average optical power minimizing amplitudes for the out-of-band carriers were found using the Sedumi 1.05 optimization toolbox [26] to solve the convex optimization problem for each symbol. Out-of-band signals chosen over the complex

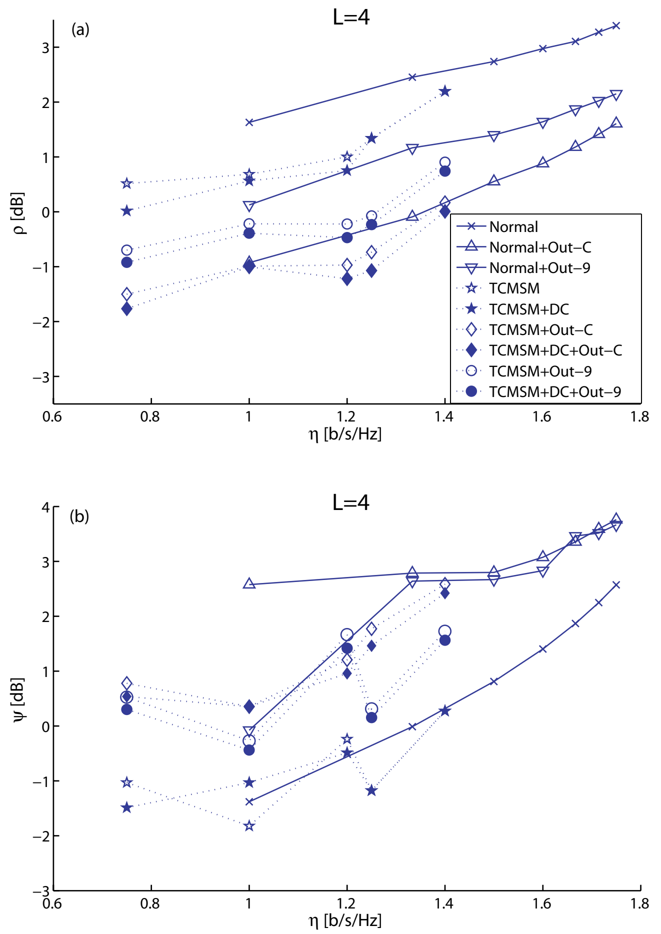

Fig. 5. Out-of-band techniques: normalized average optical power (ρ) (a) and normalized peak optical power (ψ) (b) versus bandwidth efficiency (η) using $L = 4$ out-of-band carriers for normal and in-band coded (TCMSM) systems. Note that the prefix 'Out' indicates techniques using out-of-band carriers, 'C' indicates carriers selected over the complex plane and '9' indicates amplitudes were selected from scaled 9-APSK.

plane achieved the best reduction in average optical power at the expense of greatly increased peak amplitude. Adding $L = 4$ complex-valued out-of-band carriers achieved an average optical power gain as high as 2.56 dBo, while an average optical power gain of up to 1.50 dBo is achieved using scaled 9-APSK. The peak optical power is increased by as much as 3.96 dB optical using $L = 4$ complex-valued out-of-band carriers, while selecting amplitudes over 9-APSK increases the peak optical power as much as 2.65 dBo. Note, however, that selecting carriers over the scaled 9-APSK constellation requires $1/8$ of the memory required by complex-valued out-of-band carriers. Additionally, notice that adding out-of-band carriers does not impact the detection process of normal MSM, i.e., independent detection over each in-band carrier is still possible.

Figures 5(a) and 5(b) also present the performance of $L = 4$ out-of-band carriers and in-band coding with parameters shown in Table I (for $L > 0$). The Sedumi toolbox was used once again to select out-of-band carrier amplitudes over the complex plane. When compared to a normal MSM system at the same η, combining out-of-band carriers with both in-band techniques achieved the highest gain in average optical power. An average optical power reduction of 2.63 dB optical

TABLE I

PROPERTIES OF TCMSM CODES AT EACH BANDWIDTH EFFICIENCY WITH NO OUT-OF-BAND CARRIERS AND WITH $L = 4$ OUT-OF-BAND CARRIERS

η	0.75	1.00	1.20	1.25	1.40
W	3	4	4	3	4
K	3	5	6	5	7
U	0	2	0	1	1
M	4	4	4	4	4
Sub-constellation	9-APSK	9-APSK	9-APSK	9-APSK	9-APSK
ρ [dB]					
$L = 0$	0.52	0.68	1.00	1.34	2.20
$L = 4$ 9-APSK	-0.70	-0.22	-0.22	-0.07	0.91
$L = 4$ Real	-1.50	-1.00	-0.97	-0.74	0.17
ψ [dB]					
$L = 0$	-1.03	-1.82	-0.24	-1.18	0.27
$L = 4$ 9-APSK	0.53	-0.27	1.67	0.31	1.73
$L = 4$ Real	0.78	0.35	1.21	1.77	2.58
Memory [KByte]					
$L = 4$ 9-APSK	0.1	0.5	1	0.5	2
$L = 4$ Real	1	4	8	4	16

is achieved at $\eta = 1$. Although the peak optical power is increased, this increase is smaller than that of using the out-of-band carriers without in-band trellis codes or DC detection. This is because both in-band trellis codes and the DC detection technique help to reduce the peak optical power of the selected MSM constellation points. Selecting out-of-band amplitudes from a discrete scaled 9-APSK set provides greater savings in average optical power for the same memory requirement. In our simulations, the additional memory varies between 20 to 65540 bytes for $L = 4$ scaled 9-APSK out-of-band carriers depending on η, as shown in Table I. Notice, however,that the use of in-band coding techniques does not permit independent detection of each symbol or carrier. Thus, such schemes, although providing greater average optical power efficiency, require greater complexity.

In applications where the transmitter complexity is strictly limited and little additional memory is available for the look-up table, the out-of-band techniques proposed in previous sections may become infeasible to employ. To address this problem, out-of-band carriers are applied to a subset of MSM constellation points with the largest average optical power cost. This trades average optical power reduction capabilities for a reduced memory requirement. This technique is applied to 25%, 50% and 75% of the MSM constellation points with the highest average optical power cost. It is observed that the percentage of loss in average optical power reduction and the percentage of savings in memory requirements are roughly the same in all cases. The application of this technique to other in-band systems to trade-off complexity and average optical power savings is straightforward.

Figures 6(a) and 6(b) show the average and peak optical power of a normal MSM system applied with $L = 1, 2, 3, 4, 10$ out-of-band carriers whose amplitudes are optimized over the complex plane. Notice that as L increases a larger reduction in average optical power is available at every η at the cost of greatly increased peak optical power. Thus, for a given W and K, L should be maximized to reduce ρ so long as the system is within the peak optical budget. Notice also that the incremental gain in ρ is small for $L > 4$ while ψ increases

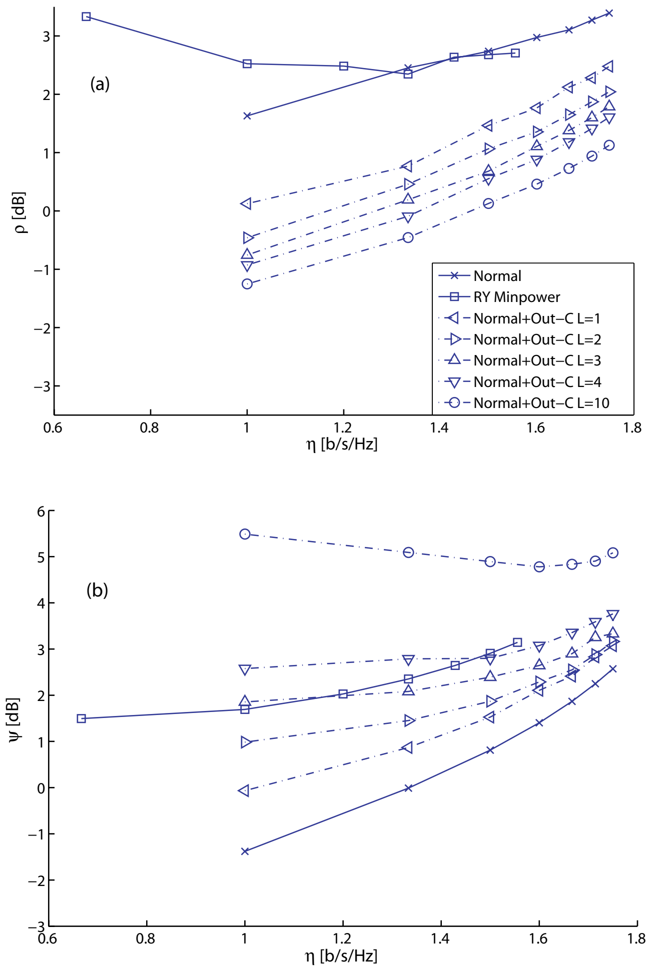

Fig. 6. Selecting L: normalized average optical power (ρ) (a) and normalized peak optical power (ψ) (b) versus η for $L = 1, 2, 3, 4, 10$ out-of-band carriers optimized over $\mathbb{C}$.

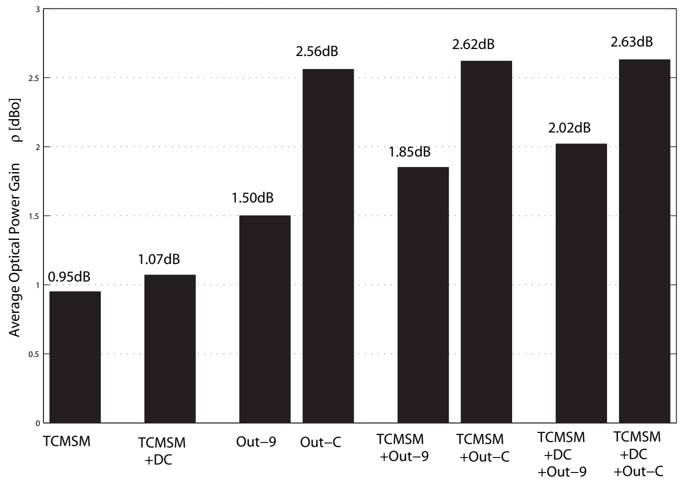

Fig. 7. Average optical power gain, ρ, over normal MSM by applying the developed techniques at $\eta = 1$. The label 'TCMSM' denotes in-band coding, 'Out' indicates $L = 4$ out-of-band carriers and 'DC' indicates the use of the DC bias technique.

greatly. Thus, the trade-off between the choice of L and the resulting ψ and ρ must be carefully balanced in any system design.

To compare and quantify the performance of the proposed techniques, a normal MSM system operating at $\eta = 1$ is taken as a baseline. The gain in average optical power for each technique in Fig. 5(a) is shown in Fig. 7. Although in-band TCMSM coding provides some gain, notice large gains in average optical power are achieved by applying out-of-band carriers to normal MSM systems, at a cost of increased peak optical power. A large peak optical power can lead to non-linear distortion at the transmitter and thus degrade the BER performance of the system. Additionally, safety limits require constraints on both the average and peak optical power of wireless optical systems, although average optical power limits dominate in nearly all cases. In general, applying out-of-band carriers is desirable when the peak optical power budget is high and in the case of a tight constraint on the peak optical power, in-band coding techniques can also be used to provide an average optical power gain for lower peak optical power. The use of the DC detection technique is also beneficial, however, less so than the previous techniques. Finally, applying all of the techniques gives the best performance at the price of additional complexity. Although the particular values of ρ will change with η, as is evident in Fig. 5(a), the above trends hold. Notice also that the gains achieved by each of the proposed techniques are not additive, i.e., the resulting gain of applying a number of techniques is less than their sum. This suggests that jointly designing in-band systems and out-of-band carriers may yield an additional reduction in the average optical power.

VI. Conclusions and Future Work

In this paper, the immense bandwidth available for wireless optical MSM channels is exploited to reduce the average optical power requirement. Out-of-band carriers are added at higher frequencies and their amplitudes optimized to reduce the average optical power requirement. Gains as high as 2.56 dBo over conventional MSM systems are realized using four out-of-band carriers. Coding over in-band carriers realizes a gain in average optical power of 0.95 dBo over uncoded systems without affecting the peak optical power at $\eta = 1$. Finally, the DC bias level is exploited at the receiver to further improve detection. Employing all the proposed techniques yields an average optical power gain of 2.63 dBo at $\eta = 1$, which corresponds to a 5.26 dB electrical power gain.

In terms of complexity, applying out-of-band carriers to normal MSM systems has the least complexity requirement among all proposed techniques. The receiver is not changed and independent symbol-by-symbol detection over each in-band carrier is maintained. However, additional complexity is required at the transmitter in the form of a lookup table. In contrast, in-band trellis coding techniques require the use of a trellis encoder at the transmitter and a sequence detector at the receiver, while the DC detection technique requires joint detection of all in-band carriers.

The work presented here serves as an introduction to the use of out-of-band carriers and coding over sequences of MSM points to reduce peak and average optical powers of indoor diffuse wireless optical channels. Additional work is required to generalize these results to a wider class of channels which are non-flat, have colored noise and are corrupted by fluorescent light interference. Joint design of these techniques is also a promising avenue of research which should be pursued to maximize the available gains. Finally, the decoding complexity of in-band schemes must be addressed and sub-optimal decoders should also be explored.

References

[1] J. M. Kahn and J. R. Barry, "Wireless infrared communications," *Proc. IEEE*, vol. 85, no. 2, pp. 265–298, Feb. 1997.

[2] S. Hranilovic, *Wireless Optical Communication Systems*. Springer, 2004.

[3] J. B. Carruthers and J. M. Kahn, "Multiple-subcarrier modulation for nondirected wireless infrared communication," *IEEE J. Select. Areas Commun.*, vol. 14, no. 3, pp. 538–546, Apr. 1996.

[4] J. A. Davis and J. Jedwab, "Peak-to-mean power control in OFDM, Golay complementary sequences, and Reed-Muller codes," *IEEE Trans. Inform. Theory*, vol. 45, no. 7, pp. 2397–2417, Nov. 1999.

[5] C. V. Chong and V. Tarokh, "A simple encodable/decodable OFDM QPSK code with low peak-to-mean envelope power ratio," *IEEE Trans. Inform. Theory*, vol. 47, no. 7, pp. 3025–3029, Nov. 2001.

[6] D. Wulich, "Reduction of peak to mean ratio of multicarrier modulation using cyclic coding," *Electron. Lett.*, vol. 32, no. 5, pp. 432–433, Feb. 1996.

[7] A. Gatherer and M. Polley, "Controlling clipping probability in DMT transmission," in *Proc. 31st Asilomar Conf. on Signals, Systems and Computers*, vol. 1, Nov. 1998, pp. 578–584.

[8] J. Tellado and J. M. Cioffi, "Efficient algorithms for reducing PAR in multicarrier systems," in *Proc. IEEE Intl. Symp on Info. Thy.*, Aug. 1998, p. 191.

[9] P. K. Frenger and N. A. B. Svensson, "Parallel combinatory OFDM signaling," *IEEE Trans. Commun.*, vol. 47, no. 4, pp. 558–567, Apr. 1999.

[10] J. Tellado and J. M. Cioffi, "PAR reduction with minimal or zero bandwidth loss and low complexity," *ANSI document,T1E1.4 Technical Subcommittee,98-173:1-12*, June 1998.

[11] J. Tellado, *Multicarrier Modulation with Low PAR: Applications to DSL and Wireless*. Kluwer, 2000.

[12] T. E. Darcie, "Subcarrier multiplexing for lightwave networks and video distribution systems," *IEEE J. Select. Areas Commun.*, vol. 8, no. 7, pp. 1240–1248, Sept. 1990.

[13] S. Hranilovic and D. A. Johns, "A multilevel modulation scheme for high-speed wireless infrared communications," in *Proc. IEEE Int. Symp. Circuits and Systems*, May 1999.

[14] R. You and J. M. Kahn, "Average power reduction techniques for multiple-subcarrier intensity-modulated optical signals," *IEEE Trans. Commun.*, vol. 49, no. 12, pp. 2164–2171, Dec. 2001.

[15] S. Teramoto and T. Ohtsuki, "Multiple-subcarrier optical communication systems with peak reduction carriers," in *Proc. IEEE GLOBECOM*, vol. 6, Dec. 2003, pp. 3274–3278.

[16] N. Kitamoto and T. Ohtsuki, "Parallel combinatory multiple-subcarrier optical wireless communication systems," *Int. J. Commun. Syst*, vol. 18, pp. 195–203, Apr. 2005.

[17] S. Teramoto and T. Ohtsuki, "Multiple-subcarrier optical communication systems with subcarrier signal-point sequence," *IEEE Trans. Commun.*, vol. 53, no. 10, pp. 1738–1743, Oct. 2005.

[18] T. Ohtsuki, "Multiple-subcarrier modulation in optical wireless communications," *IEEE Commun. Mag.*, vol. 41, no. 3, pp. 74–79, Mar. 2003.

[19] J. M. Kahn, W. J. Krause, and J. B. Carruthers, "Experimental characterization of non-directed indoor infrared channels," *IEEE Trans. Commun.*, vol. 43, no. 2/3/4, pp. 1613–1623, Feb./Mar./Apr. 1995.

[20] M. R. Pakravan, M. Kavehrad, and H. Hashemi, "Indoor wireless infrared channel characterization by measurements," *IEEE Trans. Veh. Technol.*, vol. 50, no. 4, pp. 1053–1073, July 2001.

[21] G. Ungerboeck, "Channel coding with multilevel/phase signals," *IEEE Trans. Inform. Theory*, vol. IT-28, no. 1, pp. 55–67, Jan. 1982.

[22] R.Narasimhan, M. D. Audeh, and J. M. Kahn, "Effect of electronic-ballast fluorescent lighting on wireless infrared links," *IEE Proc. Opto-electron.*, vol. 143, no. 6, pp. 347 – 354, Dec. 1996.

[23] S. Boyd and L. Vandenberghe, *Convex Optimization*. Cambridge University Press, 2004.

[24] IEEE, "Standard for binary floating point arithmetic," *ANSI/IEEE Standard 754-1985*, 1985.

[25] S. Hranilovic and F. R. Kschischang, "Optical intensity-modulated direct detection channels: signal space and lattice codes," *IEEE Trans. Inform. Theory*, vol. 49, no. 6, pp. 1385–1399, June 2003.

[26] J. F. Sturm, "Using SeDuMi 1.02, a Matlab toolbox for optimization over symmetric cones," *Optimization Methods and Software*, vol. 11-12, pp. 625–653, 1999 (see `http://sedumi.mcmaster.ca` for updates).

Weiwei Kang (S'05) received the B.Eng. degree in electrical engineering from Beijing Institute of Technology, Beijing, China in 2004 and the M.A.Sc. degree in electrical and computer Engineering from McMaster University, Hamilton, Canada in 2006. Currently, he is working toward a Masters degree in electrical engineering at the Pennsylvania State University, University Park, PA. In 2004, while studying for the B.Eng. degree, he worked in the areas of circuit and PCB design for China Electronics Corporation Wireless R&D Ltd., Beijing, China. In 2007, he worked at The Columbia Institute for Tele-Information, Columbia University as a research assistant, doing research in telecommunications sector and media industry in general. His research interests are in the areas of wireless communications, free-space optical communications and digital communication algorithms.

Steve Hranilovic (S'94-M'03-SM'08) received the B.A.Sc. degree with honours in electrical engineering from the University of Waterloo, Canada in 1997 and M.A.Sc. and Ph.D. degrees in electrical engineering from the University of Toronto, Canada in 1999 and 2003 respectively. He is an Assistant Professor in the Department of Electrical and Computer Engineering, McMaster University, Hamilton, Ontario, Canada. From 1992 to 1997, while studying for the B.A.Sc. degree, he worked in the areas of semiconductor device characterization and microelectronics for Nortel Networks and the VLSI Research Group, University of Waterloo. His research interests are in the areas of free-space and wired optical communications, digital communications algorithms, and electronic and photonic implementation of coding and communication algorithms. He is the author of the book *Wireless Optical Communications Systems* (New York: Springer, 2004). Dr. Hranilovic is a licensed Professional Engineer in the Province of Ontario. In 2006, he was awarded the Government of Ontario Early Researcher Award. He is currently the Chair of the joint IEEE Communications/Signal Processing/Information Theory Societies Chapter in the Hamilton Section.